JOURNAL OF MATERIALS SCIENCE 26 (1991) 4468–4476

Notch-sensitivity of non-linear materials

P. PURSLOW*
Muscle Biology Department, AFRC Institute of Food Research, Langford, Bristol BS18 7DY, UK

The relationships between breaking stress, σ_B, and crack length, a, and between breaking strain, ε_B, and a have been calculated for materials whose stress–strain behaviour is approximated by $\sigma = k\varepsilon^n$. The results take the form $\sigma_B \propto (a)^{-m}$ and $\varepsilon_B \propto (a)^{-p}$, where $m = n/(n+1)$ and $p = 1/(n+1)$. For $n = 1$ (the linear case), $m = p = \frac{1}{2}$. For $n > 1$, $m > \frac{1}{2} > p$ and for $n < 1$, $m < \frac{1}{2} < p$. Tests on butyl, silicone and latex rubbers as model materials confirm the applicability of the theory. The results imply that for biological materials such as skin where $n > 1$, σ_B drops off very rapidly with increasing defect size, whereas ε_B is far less dependent on a. These may be appropriate properties for a material where the degree of extension, rather than the peak loads encountered, is critical to its *in vivo* performance. For materials where $n < 1$, breaking stress is far less sensitive to crack length than fracture strain, which may be more appropriate properties for applications in which applied stress, but not strain, is critical.

1. Introduction

In considering the toughness of highly extensible biological materials such as blood vessels and skin, Gordon [1, 2] raised the general question of the effects of a non-linear stress–strain relationship on the fracture behaviour of a material. He argued that materials showing low stiffness at low extensions followed by high stiffness at high extensions would have poor shear communication of energy to a growing crack, resulting in a greater resistance to fracture despite the moderately low works of fracture that have been measured for such biological materials [3, 4].

Gordon's ideas were purely descriptive, but several workers have since analysed theoretical models of the fracture behaviour of non-linear materials. Smith [5–7] has used discrete lattice network models to predict that fracture strains [5, 6] and effective works of fracture [7] are higher if the stiffness of lattice elements increases at higher extensions than if they are linearly elastic. Kendall and Fuller [8] and Mai and Atkins [9] have analysed the effects of non-linear elasticity on the fracture behaviour of uniform, isotropic materials. Both of these papers assume the simple form of non-linear stress–strain relationship shown in Fig. 1; the power-law model, where $\sigma = k\varepsilon^n$. Such a model has been used to describe approximately the stress–strain curve of tendon and skin [10], and although it gives a far from perfect fit to the behaviour of many extensible materials, it does broadly mimic the whole range of non-linear curve shapes seen, from the r-shaped curve of many rubbers to the J-shaped case typical of biological membranes, by a simple change in the exponent n. For $n < 1$, the stress–strain curve is r-shaped, for $n > 1$ it is J-shaped, whilst $n = 1$ yields the linear case.

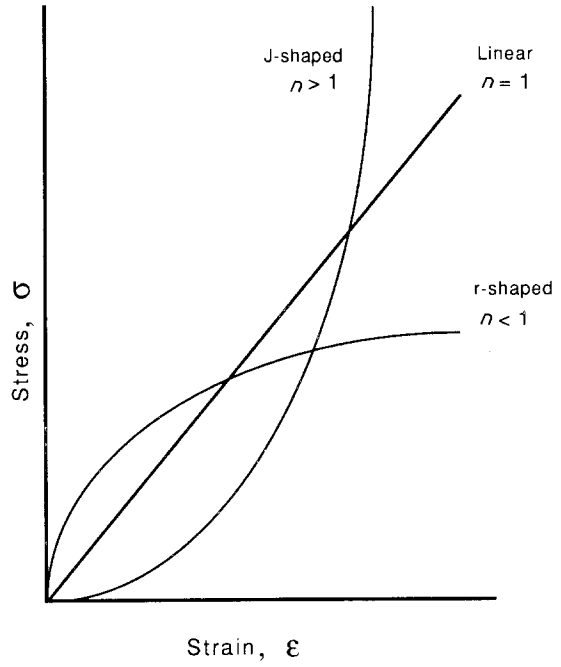

Figure 1 The power-law stress–strain model; $\sigma = k\varepsilon^n$.

Kendall and Fuller [8] analysed the effect of non-linear elasticity on the behaviour of a material in various crack propagation tests. For the trousers tear test and a lubricated cutting test they argue that the shape of the stress–strain curve has little, if any, effect on the rupture stress, and that in tensile single-edge notch tests the shape of the stress–strain curve affects the fracture stress by only a small amount. They conclude that it is not generally true that materials with J-shaped curves are more resistant to fracture. Kendall and Fuller raise an important point by questioning the criterion by which the fracture resistance of

* *Present address*: Muscle and College Research Group, University of Bristol Veterinary School, Churchill Building, Langford, Bristol BS18 7DY, UK.

0022–2461/91 $03.00 + .12

non-linear materials should be judged. They rightly point out that if biological materials are judged by work of fracture-type measurements, then their toughness is not particularly great; fracture toughness, R (the specific work of fracture as defined by Atkins and Mai [11]), is only in the range 1–20 kJ m^{-2} [2, 3, 12]. Mai and Atkins [9] make different assumptions about the energy storage in the legs of a tear test piece and predict that non-linear elasticity *does* affect the result of a tear test; they argue that under some circumstances a J-shaped stress–strain curve results in a higher tearing load than for a linear material with the same fracture toughness, R. Observations on the actual tearing behaviour of four biological materials [13] have been interpreted as supporting Mai and Atkins' assumption that the effects of energy storage in the legs of a tear test piece are not negligible. Mai and Atkins' conclusion, that biological materials with J-shaped curves are resistant to rupture because of their low stiffness at low/medium extensions, radically differs from that of Kendall and Fuller. However, they agree that the choice of definition of what is meant by non-linear materials "being more difficult to tear" is not an obvious one. Mai and Atkins ask "Do we mean bigger fracture loads at constant toughness? Or greater failure strains at constant toughness?". Comparison of the findings of these two continuum-based analyses [8, 9] to Smith's discrete lattice models [5, 6] serve to exemplify this difficulty; Smith emphasizes the effect of non-linearity on fracture strain, whereas Kendall and Fuller and Mai and Atkins argue in terms of relationships between R and fracture stress as a function of stress–strain curve shape.

The aim of this paper is to approach the question of the effects of non-linear stress–strain behaviour on fracture by explicitly examining the relationships between fracture stress and crack length, and between fracture strain and crack length, as functions of the shape of the stress–strain curve. Various sheet rubbers will be used as uniform and homogeneous model materials.

Notch sensitivity is usually described in terms of the way in which fracture stress decreases with crack length (e.g. Kelly [14]). In the analysis presented here it will be emphasized that the concomitant decrease of fracture strain with crack length can show a different pattern of notch sensitivity to that of stress in non-linear materials, and that these differences may be useful in deciding under what circumstances a non-linear material with either a higher fracture strain, or a higher fracture stress, is more "difficult" to break.

2. Theoretical analysis

A homogeneous, isotropic continuum material with a stress–strain relationship of $\sigma = k\varepsilon^n$ is assumed. The changes in elastic strain energy, U, on extension of an existing crack length a under fixed grip conditions will be considered for both notch-sensitive and notch-insensitive cases, as depicted in Fig. 2a and b, respectively. An external load, P, is applied in each case to open the crack in mode I, and the point of application of the load has a displacement u.

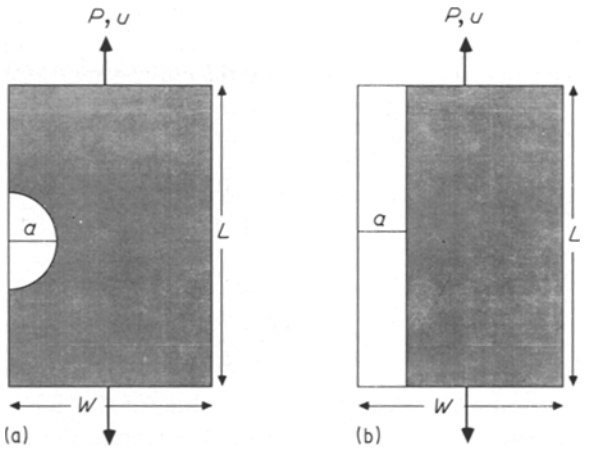

Figure 2 Single-edge notched specimens of (a) a notch-sensitive and (b) a notch insensitive non-linear material. Unshaded areas represent strain energy-free zones surrounding the notch.

2.1. Notch-sensitive case (Fig. 2a)

In this simplified model the presence of a pre-existing edge notch of length a is assumed to give rise to a stress-free zone (unshaded area) that is approximately semicircular. The total strain energy, U, in the shaded area is given by

$$U = \left(\int_0^{\varepsilon_f} \sigma \, d\varepsilon\right) \times \text{shaded volume} \quad (1)$$

where ε_f is the macroscopic failure strain, i.e.

$$U = k\frac{\varepsilon_f^{n+1}}{n+1} t\left(WL - \frac{\pi a^2}{2}\right) \quad (2)$$

where t is the specimen thickness.

The fracture toughness is given by,

$$R = -\left|\frac{dU}{dA}\right|_u \quad (3)$$

where A is the crack area ($= at$)

$$\therefore R = \frac{k\varepsilon_f^{n+1}\pi a}{n+1} \quad (4)$$

Taking R as constant

$$\varepsilon_f \propto \left(\frac{n+1}{a}\right)^{1/(n+1)} \quad (5)$$

For the linear case ($n = 1$) this yields $\varepsilon_f \propto a^{-0.5}$, as expected.

The failure stress,

$$\sigma_f = k\varepsilon_f^n \quad (6)$$

and substituting $\varepsilon_f^{n+1} = (\sigma_f/k^{(n+1/n)}$ into Equation 4 gives

$$R = k\frac{\sigma_f^{(n+1)/n}\pi a}{n+1} \quad (7)$$

Taking R as a constant

$$\sigma_f \propto \left(\frac{n+1}{a}\right)^{n/(n+1)} \quad (8)$$

For the linear case this gives $\sigma_f \propto a^{-0.5}$, in agreement with linear elastic fracture mechanics.

2.2. Notch-insensitive case (Fig. 2b)

In this case it is assumed that the unstressed zone (unshaded area) extends along the entire length, L, of the specimen for a width equal to a. Then by the same argument as above

$$U = \frac{k\varepsilon_f^{n+1} Lt(W - a)}{n + 1} \quad (9)$$

and

$$R = \frac{k\varepsilon_f^{n+1} Lt}{n + 1} \quad (10)$$

i.e. ε_f is independent of a for all values of n. It follows that the failure stress in the shaded region, the ligament failure stress, is also independent of a for all values of n, and the nominal breaking stress, σ_f, is therefore proportional to $1 - (a/W)$. This is the relationship given by Kelly [14] for notch-insensitive materials; the present analysis shows that it applies to non-linear notch-insensitive materials also.

Returning to the notch-sensitive case, the foregoing analysis predicts the following log–log relationships between σ_f and a and ε_f and a

$$\ln \sigma_f = k_1 - m \ln a \quad (11)$$

where $m = n/(n + 1)$

$$\ln \varepsilon_f = k_2 - p \ln a \quad (12)$$

where $p = 1/(n + 1)$, and where k_1 and k_2 are constants. It should be noted that $m + p = 1$, and therefore there is a reciprocal relationship in the dependence of the two log–log gradients on n, i.e. that as n increases the gradient of the $\ln \sigma_f$ versus $\ln a$ plot increases, whilst the gradient of the $\ln \varepsilon_f$ versus $\ln a$ plot concomitantly decreases, and vice versa as n decreases. This is evident in Fig. 3, which shows the values of m and p as a function of n. Only at $n = 1$ does $m = p = 1/2$. For $n < 1$, $m < 1/2 < p$ and for $n > 1$, $m > 1/2 > p$.

These forms of relationship are implicit in previous analyses of fully plastic behaviour as a non-linearly elastic problem [15–17]. However, the aim of these previous exercises was to arrive at expressions for the strain energy release rate, G, or the J-integral. The aim here is to look explicitly at the way the shape of the stress–strain relationships affects the dependence of fracture stress and fracture strain on crack length, and so it is valid to draw these points out strongly in the present analysis.

The applicability of the foregoing analysis can readily be tested by measuring σ_f and ε_f as functions of a for materials that can be adequately described by the power-law model of non-linear stress–strain behaviour, and comparing how well they fit the straight line plots predicted in Equations 11 and 12. Such tests are described below.

3. Materials and methods

Three types of rubber were obtained in large sheets of uniform thickness: butyl rubber (thickness 1.8 mm), silicone rubber (thickness 2.2 mm), and latex sheet (thickness 0.8 mm). Tensile test specimens were cut out from the sheets using a dumb-belled metal template as a guide. For butyl and silicone rubber specimens, a dumb-belled template with waisted region of width 20 mm and length 90 mm was used. For latex rubber specimens a smaller template with a waisted region 10 mm wide and 45 mm long was necessary in order to accommodate the high breaking strain of this material within the extension range of the materials testing machine used. All test specimens were cut with their long axis transverse to the roll direction of the supplied sheets, in order to avoid any possible anisotropy in the sheets. The actual widths, W, of the specimens were measured using either vernier calipers or a magnifying viewer with a calibrated eyepiece graticule. To act as targets for an infrared non-contacting extensometer used in all tensile tests, 2 mm diameter dots of self-adhesive infrared reflecting tape were placed along the mid-region of each specimen, with centre-to-centre distances of 50 mm in the case of butyl and silicone rubber specimens, and 25 mm in the case of latex specimens.

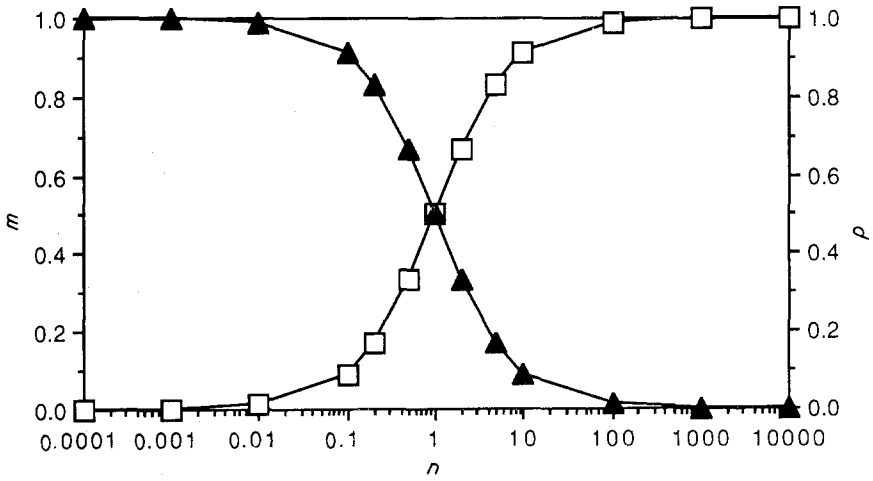

Figure 3 Predicted values of gradients m (□) and (▲) p versus values of n. As n tends to zero, m tends to zero and p to 1. As n tends to infinity, m tends to 1 and p to zero. At all values of n, $m + p = 1$.

3.1. Stress–strain and resilience measurements

In order to test the applicability of the simple power-law model of non-linear stress–strain behaviour for each material, simple tensile tests were carried out, using an Instron 6022 fitted with pneumatic grips and a J.J. Lloyd infrared non-contacting extensometer. For butyl and silicone rubber specimens, a grip-to-grip separation of 110 mm and extension rate of 220 mm min^{-1} were employed, and for latex specimens a grip separation of 45 mm and extension rate of 225 mm min^{-1} were used. Measurements of stress and strain (as measured by non-contact extensometry of the infrared-tape markers in the parallel mid-region of the specimens) were taken. A number of specimens were unloaded at the same extension rates after reaching various load levels below the breaking point of the material. Resilience, measured as the energy under the unloading curve expressed as a percentage of the energy under the loading curve, was measured as a function of peak stress during the loading cycle.

3.2. Notch-sensitivity tests

Single-edge notches of various lengths were cut up to half way across the width in the mid-region of a number of dumb-belled specimens of each material. The lengths, a, of these notches were measured by a magnifying viewer with calibrated eyepiece graticule to the nearest 0.1 mm and expressed as a ratio (a/W) of the measured width of the specimen, W. Specimens were then extended to breaking point at the same extension rates as for the unnotched, stress–strain test specimens above, and peak stresses and strain at peak stress (from the non-contacting extensometer) noted. All tensile tests were carried out at room temperature.

4. Results

4.1. Stress–strain behaviour

Fig. 4 shows log–log plots of stress–strain curves for (a) butyl, (b) silicone and (c) latex rubbers. The power-law model of non-linear behaviour predicts a straight line relationship, the gradient of the line being the value of the exponent, n. Butyl and silicone rubber can be seen to fit this model quite well, and the gradients of Fig. 4a and b correspond to n values of 0.534 and 0.682, respectively. Fig. 4c shows that the power-law model does not describe the overall stress–strain behaviour of latex rubber very well. At strains up to 400%, the log stress–log strain data fall on a good straight line (correlation coefficient 0.998) which corresponds to an r-shaped stress–strain curve, with $n = 0.563$. However, above strains of 400% the stress–strain behaviour becomes extremely J-shaped, with the log–log plot giving a very good fit in this upper region ($R^2 = 0.988$) to the power-law model with $n = 4.15$.

4.2. Notch sensitivity

Fig. 5 shows plots of ln fracture stress versus ln a/W on the left-hand side and ln fracture strain versus ln a/W on the right-hand side for (a, b) butyl, (c, d) silicone and (e, f) latex rubbers. For butyl and silicone

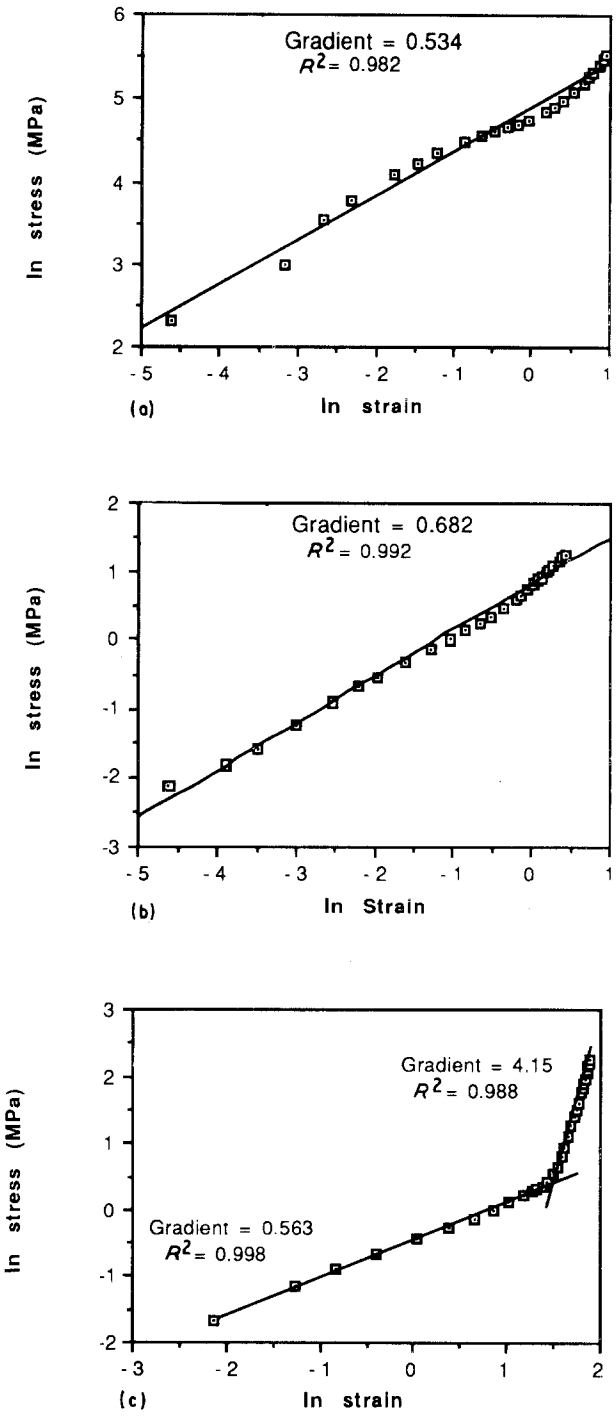

Figure 4 Log–log stress–strain plots for (a) butyl, (b) silicone and (c) latex rubbers. Straight lines drawn are regression fits of an exponential model with gradients stated; R^2 values are correlation coefficients for straight line fit.

rubbers, these relationships are very well described by straight lines ($R^2 > 0.9$ in all four cases). The absolute value of the negative gradient of the ln fracture stress versus ln a/W relationship is less than 0.5, whereas the absolute value of the negative gradient of the ln fracture strain versus ln a/W relationship is greater than 0.5 for both materials. The corresponding relationships for latex rubber are much poorer straight line fits. For latex, the absolute value of the negative gradient of the ln fracture stress versus ln a/W relationship is greater than 0.5, whereas the absolute value of the negative gradient of the ln fracture strain versus ln a/W relationship is less than 0.5.

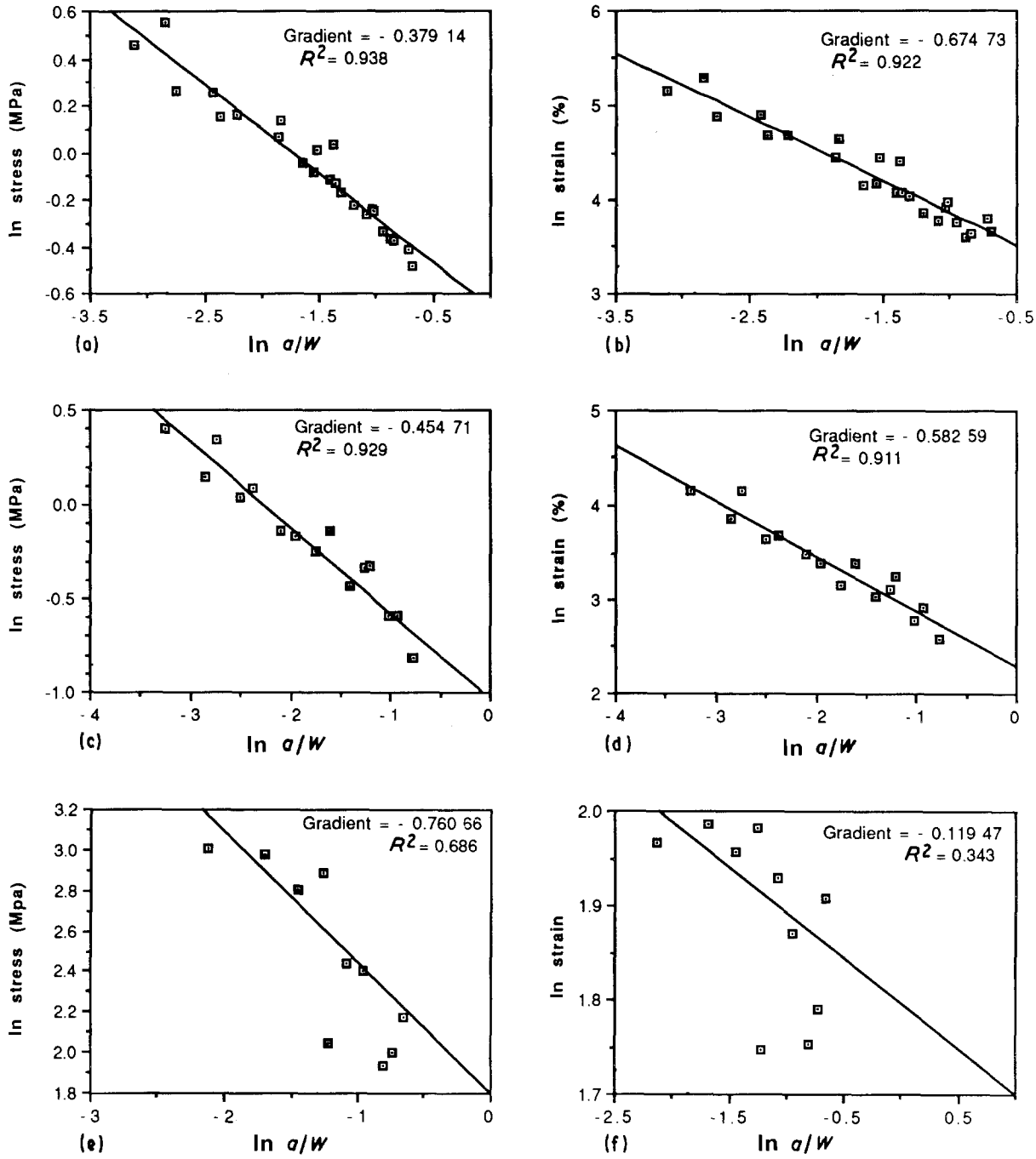

Figure 5 Log–log plots of (a, c, e) breaking stress versus a/W and (b, d, f) breaking strain versus a/W, for (a, b) butyl rubber, (c, d) silicone rubber and (e, f) latex rubber. Straight lines shown are regression fits to the data with gradients and correlation coefficients (R^2) as stated.

4.3. Resilience

Fig. 6 shows the resilience of the three rubbers as a function of peak stress in the loading cycle. In all cases, resilience falls appreciably as the material is unloaded from higher stresses.

5. Discussion

5.1. Fit between model and experimental data

The experimental results show that the theoretical analysis of fracture stresses and strains as functions of crack length, and the power-law stress–strain model on which the analysis was based, fit the behaviour of butyl and silicone rubber very well. Fig. 4 shows that the power-law model fits the stress-strain behaviour of the butyl and silicone rubbers reasonably, with correlation coefficients above 0.98. With these materials the ln σ_f versus ln a/W and ln ε_f versus ln a/W plots (Fig. 5) also give good straight line fits in accordance with Equations 11 and 12, with $R^2 > 0.9$ in each case. Table I shows a comparison between these measured gradients and those predicted by Equations 11 and 12, using the measured values of n from Fig. 4. The value of n is well below 1 for both of these materials, which the theoretical analysis predicts should result in a value for m (gradient of the ln σ_f versus ln a/W plot) below 0.5 and a value for p (gradient of the ln ε_f versus ln a/W plot) above 0.5. Table I shows that this is the case, and moreover the actual values of m and p match the predicted values well. The analysis therefore appears to be applicable to these materials.

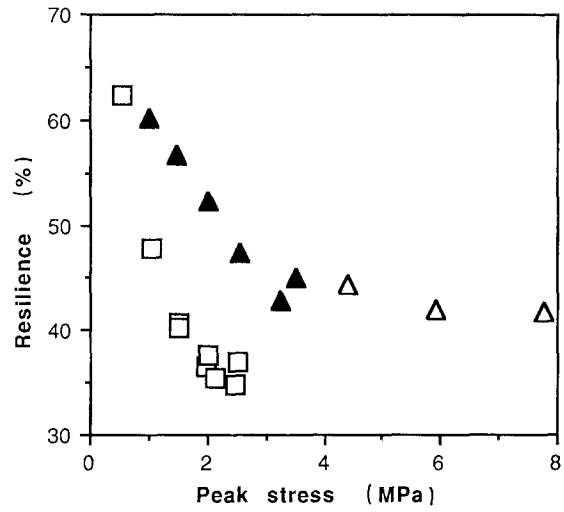

Figure 6 Resilience (energy under unloading curve as a percentage of energy under loading curve) versus peak stress reached in loading cycle. (▲) Silicone, (□) butyl and (△) latex rubbers.

Latex rubber is less well described by the power-law stress–strain model and also matches the non-linear notch sensitivity analysis less well. At extensions up to approximately 400% latex has an r-shaped stress–strain curve well described by a power-law model with $n = 0.563$ ($R^2 = 0.998$ for this lower region only). At higher extensions the stress–strain curve sweeps rapidly upwards in a J-shaped form; this upper segment of the curve is well described by a power-law model with $n = 4.15$ ($R^2 = 0.988$). Visual observations of the edge-notched latex specimens suggested that the bulk of the test piece was operating in this upper region of the curve immediately prior to rupture. The value of $n = 4.15$ was therefore taken to be the most appropriate. Despite the high scatter in the ln σ_f versus ln a/W and ln ε_f versus ln a/W plots for latex, their gradients did show the trend predicted by the theoretical analysis, with $m > 0.5 > p$, as shown in Table I. The predicted values for m and p are, in fact, moderately close to their predicted values, but no great emphasis can be placed on this due to the high scatter in Fig. 5 for this material. It may be that other forms of stress–strain relationship would better describe the properties of this material. For example, Atkins and Mai [11] proposed a sinh or cosh relationship. The power-law model was chosen here only for its simplicity and in order to relate this work to previous papers [8, 9]; any integrable function could be substituted in the analysis given in Section 2.

5.2. Assumptions of the present analysis

There is a general point to be made about the assumptions in the present analysis of an isotropic material with a constant toughness, R, and J-shaped stress–strain behaviour at high uniaxial extensions. Mullins and Thomas [18] point out that, in general, very highly extensible rubbers show such a J-shaped upper region. This is because high strains align initially random polymer chains along the stretching direction in an increasingly non-Gaussian distribution. Natural rubbers such as latex also tend to strain-crystallize [19]. This alignment of initially random polymer networks results in strain-induced anisotropy in materials that are initially isotropic. Initially random networks of collagen molecules in dilute gelatin gels also show J-shaped stress-strain behaviour [20] which is thought to be due to strain-induced reorientation of the molecular network. Thus it may be the general case that J-shaped stress–strain behaviour arising from reorientation of polymer networks inevitably means that, in such materials at high extensions near to breaking point, anisotropy must be developed even from initially isotropic conditions. This would complicate the simple, isotropic, analysis presented here.

Strain-induced reorientation of collagen fibres in biological membranes such as blood vessel wall and skin have long been recognized as the cause of their J-shaped stress–strain curves. Bigi *et al.* [21] and Roveri *et al.* [22] have quantitatively matched changes in the angular distribution of collagen fibre networks to increasing stiffness on extension in a collagenous tissue. As well as undoubtedly producing increased anisotropy in these materials, this strain-induced reorientation may produce an increased fracture toughness local to the crack tip; Purslow *et al.* [23] have shown that the stress and strain fields around a crack tip in biaxially stretched blood vessel wall act to align strongly collagen fibre bundles across the crack tip path, so presumably making further propagation more difficult. These features of J-shaped stress–strain behaviour of biological materials may generally reduce the applicability of so simple an analysis as presented here, but the present work does at least give some broad indications of the trend in notch-sensitivity to be expected from non-linear materials. Another criticism of the simplified models presented here concerns the assumption in the notch-insensitive case of a homogeneous, isotropic material. In practice, notch-insensitivity is usually only displayed by anisotropic composite structures, and it may well be that only heterogeneous and anisotropic structures can show true notch-insensitivity. However, when looking at biological tissues it is obvious that these materials are, in fact, complex composite structures at many levels of organization, from the macroscopic down to the molecular.

TABLE I Fit between model and observed notch sensitivity

Material	n-value	Gradient m		Gradient p	
		Predicted	Observed	Predicted	Observed
Butyl	0.534	0.341	0.379	0.621	0.675
Silicone	0.682	0.405	0.458	0.595	0.583
Latex	4.15	0.806	0.761	0.194	0.119

The theoretical analysis in Section 2 implicity assumes perfectly elastic behaviour. Fig. 6 shows that all the materials tested here are less than perfectly elastic, especially at high strains. The fact that the analysis presented does reasonably describe the notch-sensitivity of these non-linear materials may therefore be fortuitous, but it is worth pointing out that previous analyses [15–17] of fracture energies of fully plastic behaviour have been based on a model of a fully elastic non-linear stress–strain curve, and that such an approach has been found to have validity as long as the load–extension relationship of a cracked specimen was a monotonically increasing curve [16]. In general terms, then, although the assumptions of a homogeneous, isotropic material showing perfect elastic energy storage are not strictly applicable to real materials of an extensible, non-linear nature, it seems nevertheless that the analysis presented here has some degree of predictive validity and usefulness. It should be pointed out that this paper provides an experimental test of non-linear theory; previous analyses [1–7] were purely theoretical.

5.3. Relationship of present analysis to previous work

In their analysis of fracture in single-edge notched specimens of non-linear materials, Kendall and Fuller [8] use the Rivlin and Thomas [24] analysis for rubbers, i.e. that $R = 2K(\lambda)a\,W_0$. W_0 is the remote strain energy density in the test piece, which Kendall and Fuller calculate in the same form as Equation 4 here. The factor K is a function of extension ratio λ which Kendall and Fuller take as $K(\lambda) = k/\lambda^{0.5}$ from the work of Lake [25]. The value of k is just below π. Greensmith [26] shows that $K(\lambda)$ decreases from a value of about 3 at small strains to just below 2 at 200% extension, and suggests that at small strains K should theoretically be close to π for an edge notch. Equation 4 here is equivalent to Kendall and Fuller's analysis except for π here being subsituted for the $2K(\lambda)$ term of Kendall and Fuller's result. The present analysis extends Kendall and Fuller's analysis specifically in discussion of concomitant changes in failure strains as well as changes in failure stress as n varies, and the possible significance of this, as discussed below.

Smith [6] models a non-linear shear communication between parallel elements in a material by considering a linear stress–strain relation that has a positive gradient only above a critical strain. Below this strain the gradient is zero, i.e. there is no resistance to extension. He argues that a more J-shaped curve, modelled by an increasing value of the critical strain, leads to a higher failure strain. This finding is similar to Smith's earlier analysis [5] where higher macroscopic failure strains result from increasing the ratio of the stiffness in the highly strained crack tip region to the stiffness further along the lattice chains of a two-dimensional lattice model. Both of these results are not inconsistent with the present analysis, which predicts that an increase in n results in an increased ε_f at a given crack length. However, Smith's interpretation [5, 6] that such increases in failure strain are indicative of increasing resistance to crack propagation is open to question; as shown here, a model can be erected where increasingly J-shaped stress–strain behaviour can lead to a higher fracture strain at a given crack length whilst fracture toughness, R, remains constant. Whilst it is of interest to hypothesize on the possible effects of increasing non-linear effects on R, it is a practical point that real materials vary in stress–strain curve shape only because of variations in structure and in structural mechanisms of deformation, and such variations have their own role in determining the toughness of a material. When considering a real (and possibly non-linear) material with a given toughness, the analysis presented here has practical significance in that it predicts the fracture stress and strain of a cracked specimen. The assumption of constant R also makes the present work not directly comparable to that of Smith [7], where he finds that a J-shaped stress–strain behaviour increases the effective work of fracture of a two-dimensional lattice model by widening the lattice-trapping regime.

It is interesting to note that Smith [7] concludes that, although effective, macroscopic values of R may be affected by non-linearity on this non-continuum model, conventional measurements of the critical stress intensity factor, K_c, could still be valid. It is an obvious consequence of the analysis presented here that K_c, although a constant for a linear material, characteristic of its toughness, is not a constant for non-linear materials. In the linear case, because fracture stress is proportional to the square root of crack length, then

$$\sigma_f(\pi a)^{1/2} = \text{constant} = K_c \qquad (13)$$

But it has been shown above that when $n \neq 1$ then $\sigma_f \neq (a)^{-0.5}$. For the non-linear case

$$\sigma_f a^{\frac{n}{(n+1)}} = \text{constant} \quad (\text{constant} = \Psi_c, \text{ say}) \qquad (14)$$

and this is obviously borne out by the experimental data in Fig. 5, where all of the ln σ_f versus ln a/W plots have gradients that deviate from -0.5 in the predicted manner. In general $\sigma_f\ a^{1/2}$ will be a non-constant function of a for all n except $n = 1$. Therefore, whilst Ψ_c is a generally applicable (linear and non-linear) stress intensity factor, K_c as conventionally defined in Equation 13 is valid only for the linear case and is not constant for non-linear cases, contrary to Smith's interpretation [7].

5.4. Significance – strategies for extension versus load-limited applications

The arguments presented here reinforce the opinions of Kendall and Fuller [8] and Mai and Atkins [9] that great care must be exercised when interpreting any effects of non-linearity in relation to the "difficulty" of breaking a material. As the present analysis clearly shows, non-linear effects which raise the failure strain for a given crack length at constant toughness may concomitantly decrease the failure stress. In general, fracture stress and strain do not follow identical relationships with crack length as expected from linear

theory, but are affected in some reciprocal way to each other by increasing non-linearity in the stress–strain relationship. These effects can be independent of any differences in the toughness as defined by R, as shown by the present analysis.

It is possible, on the basis of these different sensitivities of fracture stress and fracture strain to crack length, to conceive of "design strategies" in terms of the stress–strain behaviour of a material in order to make fracture more difficult under different conditions of test or use. Consider Fig. 7. Fig. 7a shows the stress–strain curves up to fracture as a function of increasing crack length in the case where $n > 1$, i.e. J-shaped behaviour. Analysis predicts, and experimental results show, that as a increases, breaking stress drops off very rapidly, so that for a lengthy crack the breaking stress has fallen very considerably from that of an unnotched sample. However, the diminution in failure strains resulting from the same increase in crack length is much smaller. This type of behaviour would be a good strategy to resist fracture in service conditions that were entirely displacement controlled. For example, the skin covering a knee joint is strained by an amount fixed by the flexure of the knee joint. If the skin is cut or torn, then it is desirable that the tear does not propagate whenever the knee bends, and experience tells us that we can walk and run normally without the likelihood of knee flexure resulting in the propagation of a cut. Because the failure strain of highly J-shaped materials such as skin is relatively insensitive to the presence of notches, this analysis shows why tears in the skin over a knee joint may have to be very large indeed before the fracture strain of the "cracked" skin would drop sufficiently for it to be in danger of tearing, so long as it is the extension of the skin, and not the resulting loads generated, that are the critical factor.

Fig. 7b shows the stress–strain curves to fracture of an r-shaped material ($n < 1$) as crack length increases. In this case, an increase in a brings about a large decrease in the fracture strain, but only a small decrease in the fracture stress. By a reciprocal argument, materials with r-shaped stress–strain curves may well be better suited than linear or J-shaped materials to load-defined applications. In terms of biological materials, some hard tissues such as bone [27] and shells of molluscs [28] can have this sort of stress–strain relationship, although a non-reversible one in these instances. Antler has a reversible r-shaped stress–strain curve up to approximately 3% extension, but increasing irreversibility occurs at strains up to 8% [29].

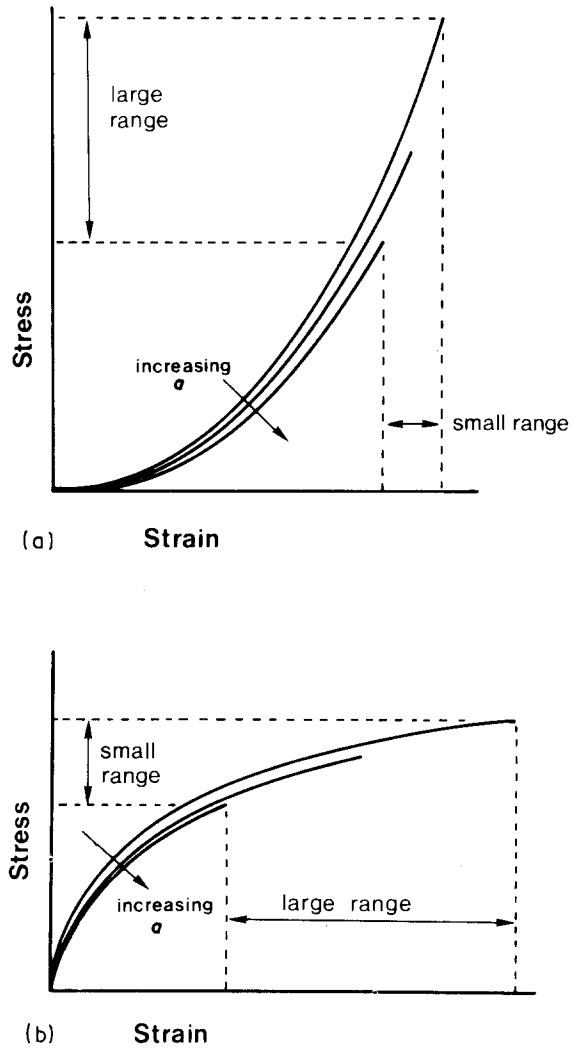

Figure 7 Stress–strain curves to fracture for (a) J-shaped materials ($n > 1$) and (b) r-shaped materials ($n < 1$). Increasing crack length results in greater decreases in fracture stress than fracture strain in (a), and vice versa in (b).

Acknowledgements

Professor A. G. Atkins is thanked for helpful discussions of this work and for advice on the line of argument in Section 2.

References

1. J. E. GORDON, in "Structures" (Penguin, Harmonsworth, 1978).
2. *Idem.*, in "The Mechanical Properties of Biological Materials", edited by J. F. V. Vincent and J. D. Currey (Cambridge University Press, 1980).
3. P. P. PURSLOW, *J. Mater. Sci.* **18** (1983) 3591.
4. *Idem., J. Biomech.* **16** (1983) 947.
5. E. SMITH, *J. Mater. Sci. Lett.* **4** (1985) 338.
6. *Idem., J. Mater. Sci.* **22** (1987) 867.
7. *Idem., Mater. Sci. Engng* **A112** (1989) 25.
8. K. KENDALL and K. N. G. FULLER, *J. Phys. D. Appl. Phys.* **20** (1987) 1596.
9. Y. W. MAI and A. G. ATKINS, *ibid.* **22** (1989) 48.
10. H. R. ELDEN, *Collagen Currents* **7** (1968) 228.
11. A. G. ATKINS and Y. W. MAI, "Plastic and Elastic Fracture" (Ellis Horwood, Chichester, 1985) pp. 80, 154.
12. P. P. PURSLOW, PhD thesis, University of Reading (1980).
13. *Idem., J. Phys. D. Appl. Phys.* **22** (1989) 854.
14. A. KELLY, in "Strong solids" (Clarendon Press, Oxford, 1966) p. 159.
15. J. R. RICE and G. F. ROSENGREN, *J. Mech. Phys. Solids* **16** (1968) 1.
16. J. W. HUTCHINSON, *ibid.* **16** (1968) 13.
17. J. G. WILLIAMS, in "Fracture mechanics of polymers" (Ellis Horwood, Chichester, 1984) p. 51.
18. L. MULLINS and A. G. THOMAS, in "The Chemistry and Physics of Rubber-like Substances", edited by L. Bateman (Maclaren, London) p. 154.
19. E. H. ANDREWS, *J. Appl. Phys.* **32** (1961) 542.
20. W. G. COBBETT and A. G. WARD, *Rheol. Acta* **7** (1968) 217.

21. A. BIGI, A. RIPAMONTI, N. ROVERI, G. JERONIMIDIS and P. P. PURSLOW, *J. Mater. Sci.* **16** (1981) 2557.
22. N. ROVERI, A. RIPAMONTI, C. PULGA, G. JERONIMIDIS, P. P. PURSLOW, D. VOLPIN and L. GOTTE, *Makromol. Chem.* **181** (1980) 1999.
23. P. P. PURSLOW, A. BIGI, A. RIPAMONTI and N. ROVERI, *Int. J. Biol. Macromol.* **6** (1984) 21.
24. R. S. RIVLIN and A. G. THOMAS, *J. Polym. Sci.* **10** (1953) 291.
25. G. J. LAKE, Malaysian Rubber Producers Research Association Reprint No. 0207.
26. H. W. GREENSMITH, *J. Appl. Polym. Sci.* **7** (1963) 993.
27. J. D. CURREY, *Clin. Orthop.* **73** (1970) 210.
28. *Idem.*, in "The Mechanical Properties of Biological Materials", edited by J. F. V. Vincent and J. D. Currey (Cambridge University Press, 1980).
29. *Idem.*, personal communication.

Received 23 May
and accepted 27 June 1990